α-Synuclein binds large unilamellar vesicles as an extended helix†

Adam J. Trexler and **Elizabeth Rhoades**[*]

Department of Molecular Biophysics and Biochemistry, Yale University, P.O. Box 208114, New Haven, CT 06520.

Abstract

Interactions between the synaptic protein α-Synuclein and cellular membranes may be relevant both to its native function as well as its role in Parkinson's disease. We use single molecule Förster resonance energy transfer to probe the structure of α-Synuclein bound to detergent micelles and lipid vesicles. We find evidence that it forms a bent-helix when bound to highly curved detergent micelles, whereas it binds more physiological 100 nm diameter lipid vesicles as an elongated helix. Our results highlight the influence of membrane curvature in determining α-Synuclein conformation, which may be important for both its normal and disease-associated functions.

α-Synuclein (AS) is the primary protein constituent of cytoplasmic Lewy bodies and Lewy neurites that are the pathological hallmark of Parkinson's Disease (PD)[1, 2]. Although it is strongly implicated in disease progression [3] the precise role of AS in PD is unclear. The native function of AS is also poorly understood, although evidence suggests that it may play a role both in maintaining neuronal plasticity and in the regulation of synaptic vesicle recycling [4, 5].

AS is disordered in solution[6] but undergoes a conformational change to an α-helical structure upon association with negatively charged membranes[7, 8]. A number of *in vitro* studies have characterized the interactions of AS both with detergent micelles and lipid membranes (reviewed in [9]). However, there is conflicting evidence as to whether AS demonstrates preferential affinities for specific phospholipids[7−12] as well as if association with lipids inhibits or promotes AS aggregation or oligomerization[12−16]. A further matter of debate is the configuration of micelle or vesicle bound AS, with contrasting models proposing either an extended, continuous helix[17−20] or two anti-parallel, non-interacting helices[21−24], with an unstructured loop region between residues ~40–45 (Figure 1). Characterizing these conformations is of great interest, as membrane-bound structures may be pertinent both to native and disease-associated functions.

Here we use single molecule Förster resonance energy transfer (FRET) to probe the helical structure of AS bound to SDS micelles and large unilamellar vesicles (LUVs). In FRET, the energy transfer efficiency (ET_{eff}) is dependent upon the distance between donor and acceptor fluorophores to the sixth power [25]. In single molecule studies of protein conformations, each protein is labeled with a donor and an acceptor fluorophore. Photon bursts from the labeled

SUPPORTING INFORMATION PARAGRAPH

Experimental details of protein expression and labeling; single molecule measurements and analysis; anisotropy and circular dichroism controls. This material is available free of charge via the internet at http://pubs.acs.org..

proteins are collected as they diffuse through a diffraction-limited excitation volume. ET_{eff} is calculated as: $ET_{eff}= I_a°/(I_a°+\gamma I_d°)$, where $I_a°$ and $I_d°$ are the photon counts on the acceptor and donor channels, respectively, corrected for background and signal bleed-through; γ accounts for properties of the instrument and fluorophores as detailed in the SI(26). An ET_{eff} is calculated for each burst and a histogram is compiled of the individual values.

Single and double cysteine mutants of wild-type AS were engineered to allow for site-specific labeling with maleimide fluorophores. Mutations were introduced at residues S9, T33, and T72 and AS-S9C-T72C, AS-T33C-T72C, and AS-S9C-T33C double mutants were used for FRET measurements (Figure 1).The protein was expressed and purified as described previously (27), then labeled with donor (Alexa 488 maleimide) and acceptor (Alexa 594 maleimide) fluorophores generally following the protocol provided by the manufacturer (Invitrogen: SI for details). It was confirmed by circular dichroism and fluorescence correlation spectroscopy that the presence of the fluorophores did not significantly perturb binding of AS to either SDS micelles or LUVs ((27) and SI for details). Steady state anisotropy measurements showed a low anisotropy value for both fluorophores at all mutation sites, indicating free rotation of the fluorophores with minimal artifacts in the ET_{eff} calculations (SI for details). The expected R_o for these fluorophores is ~54 Å(28).

Measurements were made with ~90 pM AS in buffer (20mM Tris, 30mM NaCl, pH 7.4) or in the presence of sodium dodecyl sulfate (SDS) (40 mM) or ~100 nm diameter 1-palmitoyl-2-oleoyl-phosphatidylserine (POPS) LUVs (160 µM lipid). These conditions were chosen such that not only is all the protein expected to be bound, but that only a single protein is bound per micelle or vesicle. NMR studies have shown that 40 mM SDS is sufficient to fully bind 100 µM AS (29), and thus is in great excess for the 90 pM protein used in this study The partition coefficient of fluorescently labeled wild-type AS for 100% POPS LUVs has been measured as ~3µM (lipid concentration) under solution conditions similar to the ones we use (27). Based on this number, we expect >98% of the protein to be bound and we calculate the vesicle:protein ratio to be >20:1. POPS was chosen for the work discussed here both because AS binds to it with high affinity and because phosphatidylserine comprises up to 30% of the lipid content of cellular membranes. However, other studies indicate that lipid composition may influence the membrane-bound conformation of AS (13), and thus this topic is an area of ongoing investigation in our group.

The resulting ET_{eff} histograms for AS-S9C-T72C are plotted in Figure 2. In buffer, the ET_{eff} peak value is 0.64 and shifts to 0.86 in the presence of SDS micelles (Figure 2A). These ET_{eff} values are roughly what was expected based on the bent-helix model, where residues 9 and 72 are brought into close proximity upon helix formation (Figure 1) and exhibit the same general trends as the ET_{eff} values measured for SDS micelle bound AS in another recent study which used a different acceptor fluorophore(30). While there are difficulties associated with calculating distances from ET_{eff}, due to uncertainties in contribution of the fluorophore linkers (31) both of our measured ET_{eff} values are in good agreement with what is predicted for a random coil (in solution) and for the bent-helix (on SDS micelles) (21).

However, when bound to both 50 and 100 nm diameter LUVs (data not shown), the ET_{eff} drops effectively to 0, indicating that the distance between the fluorophores is either too great to be measured or is a very low value ($ET_{eff}< 0.1$), such that we are unable to distinguish it from the $ET_{eff}=0$ peak that arises from mislabeled proteins (see SI for discussion). In a single, unbroken helix, the separation between residues 9 and 72 is expected to be between 9 and 10 nm, at the limit of the distance range that should be detectable by our donor-acceptor fluorophores (SI for details). These data provide further evidence that all of the protein is either micelle or vesicle bound during our measurements. If a significant fraction of AS remains free in the micelle or

LUV experiments, the free subpopulations would be observed with $ET_{eff} = 0.64$ and we do not find any evidence of unbound protein in our histograms.

The AS-T33C-T72C construct was designed to further probe the structure of the vesicle bound protein (Figure 1). The ET_{eff} of AS-T33C-T72C bound to SDS micelles ($ET_{eff} = 0.81$) was higher than that of the free protein ($ET_{eff} \sim 0.72$) indicating closer contact between the donor and acceptor fluorophores (Figure 3A & B). We are also able to observe a clear $ET_{eff} = 0.57$ peak for LUV bound AS-T33C-T72C (Figure 3C). This shift to smaller ET_{eff} as compared to the micelle bound protein suggests that residues 33 and 72 are further separated when bound to LUVs, supporting our prediction that AS forms an elongated helix on LUVs.

As a control, the helical region probed by AS-S9C-T33C was expected to be independent of whether the overall conformation was bent or extended and the measured ET_{eff} values for micelle and LUV samples were essentially indistinguishable ($ET_{eff} \sim 0.8$; Figure S4).

This study establishes the viability of single molecule FRET for characterizing membrane-bound conformations of AS. There is a fair amount of discussion in the literature about the meaning of the width of single molecule ET_{eff} histograms. Broadening is often attributed to dynamics that are slow on the timescale of diffusion (32). While AS is disordered in solution and thus expected to be highly dynamic, long-range contacts exist between the C-terminus and the central region of the protein (33) which may restrict motion and slow dynamics. For the AS constructs studied here, the ET_{eff} distributions in buffer are wider than the micelle or LUV bound ones ($\sigma_{buffer} = 0.27$ and $\sigma_{micelle} = 0.17$ for AS-S9C-T72C and $\sigma_{buffer} = 0.31$, $\sigma_{micelle} = 0.21$, and $\sigma_{LUV} = 0.24$ for AS-T33C-T72C). The helical micelle and LUV bound states are more restricted conformations, resulting in reduced dynamic motion and narrower ET_{eff} histograms. However, we note that both the micelle and LUV bound distributions are still rather wide for the AS-T33C-T72C construct. This may be due to the probe at residue 33 which is close to the loop region of the bent helix; this region is thought to remain disordered (17) even while the overall conformation of the protein adopts an extended helix. The T33C probe may reflect increased dynamics of this region of both the micelle and the vesicle bound protein (34), either due to fraying of the helix or the mobility of adjacent residues. We also cannot eliminate the possibility that peak broadening results from AS sampling two or more specific conformations with close mean ET_{eff} values that are not resolved in our measurements.

A number of recent studies highlight the ongoing debate regarding the physiologically relevant form, bent or extended membrane-bound helix, of AS. Our findings are in good agreement with two recent reports - an ESR study of AS bound to lipid vesicles and bicelles (19) and a combined EPR and molecular dynamics simulation study of AS bound to lipid vesicles (20) – both of which find that AS binds to these model membranes in an extended helix. While there is a strong argument to be made in favor of lipid bilayers as a much more physiologically relevant model system, a third study of SDS-induced folding of AS also concluded that at high detergent concentrations, where rod-like micelles are expected to dominate over highly-curved spherical ones, AS populates an alternative conformation, suggested to be the elongated helix (35). Ours, and these other recent findings, are in direct contrast to a second recent EPR study which found evidence for a bent-helix on ~20–30 nm diameter vesicles(23).

This study emphasizes the role of the physical parameters of the membrane mimetic, particularly curvature, in determining the conformation of membrane-bound AS. Membrane binding is closely associated with both AS native function and its pathology in PD. In PD, it is hypothesized that AS may bind and permeabilize the plasma membrane(36). On the scale of the helical region of AS, the plasma membrane is a low curvature surface and thus the mechanism of membrane disruption could involve the elongated helical form of AS. However, the native function of AS is thought to involve binding to much more highly curved synaptic

vesicles. Thus both membrane-bound structures we observe may be important to understanding AS. It remains to be determined precisely how vesicle curvature mediates the conformational switch from bent to elongated helix and how these structures relate to the native function of AS and its role in PD

Supplementary Material

Refer to Web version on PubMed Central for supplementary material.

Acknowledgments

REFERENCES

1. Goedert M. Nat. Rev. Neurosci 2001;2:492–501. [PubMed: 11433374]
2. Ueda K, Fukushima H, Masliah E, Xia Y, Iwai A, Yoshimoto M, Otero DAC, Kondo J, Ihara Y, Saitoh T. Proc. Natl. Acad. Sci 1993;90:11282–11286. [PubMed: 8248242]
3. Cookson MR. Annu. Rev. Biochem 2005;74:29–52. [PubMed: 15952880]
4. George JM, Jin H, Woods WS, Clayton DF. Neuron 1995;15:361–372. [PubMed: 7646890]
5. Lotharius J, Brundin P. Hum. Mol. Genet 2002;11:2395–2407. [PubMed: 12351575]
6. Weinreb PH, Zhen WG, Poon AW, Conway KA, Lansbury PT. Biochemistry 1996;35:13709–13715. [PubMed: 8901511]
7. Davidson WS, Jonas A, Clayton DF, George JM. J. Biol. Chem 1998;273:9443–9449. [PubMed: 9545270]
8. Jo EJ, McLaurin J, Yip CM, St George-Hyslop P, Fraser PE. J. Biol. Chem 2000;275:34328–34334. [PubMed: 10915790]
9. Beyer K. Cell Biochem. Biophys 2007;47:285–299. [PubMed: 17652776]
10. Narayanan V, Scarlata S. Biochemistry 2001;40:9927–9934. [PubMed: 11502187]
11. Perrin RJ, Woods WS, Clayton DF, George JM. J. Biol. Chem 2000;275:34393–34398. [PubMed: 10952980]
12. Zhu M, Li J, Fink AL. J. Biol. Chem 2003;278:40186–40197. [PubMed: 12885775]
13. Zakharov SD, Hulleman JD, Dutseva EA, Antonenko YN, Rochet JC, Cramer WA. Biochemistry 2007;46:14369–14379. [PubMed: 18031063]
14. Lee HJ, Choi C, Lee SJ. J. Biol. Chem 2002;277:671–678. [PubMed: 11679584]
15. Zhao HX, Tuominen EKJ, Kinnunen PKJ. Biochemistry 2004;43:10302–10307. [PubMed: 15301528]
16. Zhu M, Fink AL. J. Biol. Chem 2003;278:16873–16877. [PubMed: 12621030]
17. Bussell R, Eliezer D. J. Mol. Biol 2003;329:763–778. [PubMed: 12787676]
18. Jao CC, Der-Sarkissian A, Chen J, Langen R. Proc. Natl. Acad. Sci. U. S. A 2004;101:8331–8336. [PubMed: 15155902]
19. Georgieva ER, Ramlall TF, Borbat PP, Freed JH, Eliezer D. J. Am. Chem. Soc 2008;130:12856–12857. [PubMed: 18774805]
20. Jao CC, Hegde BG, Chen J, Haworth IS, Langen R. Proc. Natl. Acad. Sci. U.S.A 2008;105:19666–19671. [PubMed: 19066219]
21. Borbat P, Ramlall TF, Freed JH, Eliezer D. J. Am. Chem. Soc 2006;128:10004–10005. [PubMed: 16881616]
22. Chandra S, Chen XC, Rizo J, Jahn R, Sudhof TC. J. Biol. Chem 2003;278:15313–15318. [PubMed: 12586824]
23. Drescher M, Veldhuis G, van Rooijen BD, Milikisyants S, Subramaniam V, Huber M. J. Am. Chem. Soc 2008;130:7796–7797. [PubMed: 18512917]
24. Ulmer TS, Bax A, Cole NB, Nussbaum RL. J. Biol. Chem 2005;280:9595–9603. [PubMed: 15615727]

25. Forster T. Ann. Phys.-Berlin 1948;2:55–75.

26. Ha TJ, Ting AY, Liang J, Deniz AA, Chemla DS, Schultz PG, Weiss S. Chem. Phys 1999;247:107–118.

27. Rhoades E, Ramlall TF, Webb WW, Eliezer D. Biophys. J 2006;90:4692–4700. [PubMed: 16581836]

28. Schuler B, Lipman EA, Eaton WA. Nature 2002;419:743–747. [PubMed: 12384704]

29. Eliezer D, Kutluay E, Bussell R, Browne G. J. Mol. Biol 2001;307:1061–1073. [PubMed: 11286556]

30. Veldhuis G, Segers-Nolten I, Ferlemann E, Subramaniam V. ChemBioChem. 2008 early view.

31. McCarney ER, Werner JH, Bernstein SL, Ruczinski I, Makarov DE, Goodwin PM, Plaxco KW. J. Mol. Biol 2005;352:672–682. [PubMed: 16095607]

32. Nir E, Michalet X, Hamadani KM, Laurence TA, Neuhauser D, Kovchegov Y, Weiss S. J. Phys. Chem. B 2006;110:22103–22124. [PubMed: 17078646]

33. Dedmon MM, Lindorff-Larsen K, Christodoulou J, Vendruscolo M, Dobson CM. J. Am. Chem. Soc 2005;127:476–477. [PubMed: 15643843]

34. Bortolus M, Tombolato F, Tessari I, Bisaglia M, Mammi S, Bubacco L, Ferrarini A, Maniero AL. J. Am. Chem. Soc 2008;130:6690–6691. [PubMed: 18457394]

35. Ferreon ACM, Deniz AA. Biochemistry 2007;46:4499–4509. [PubMed: 17378587]

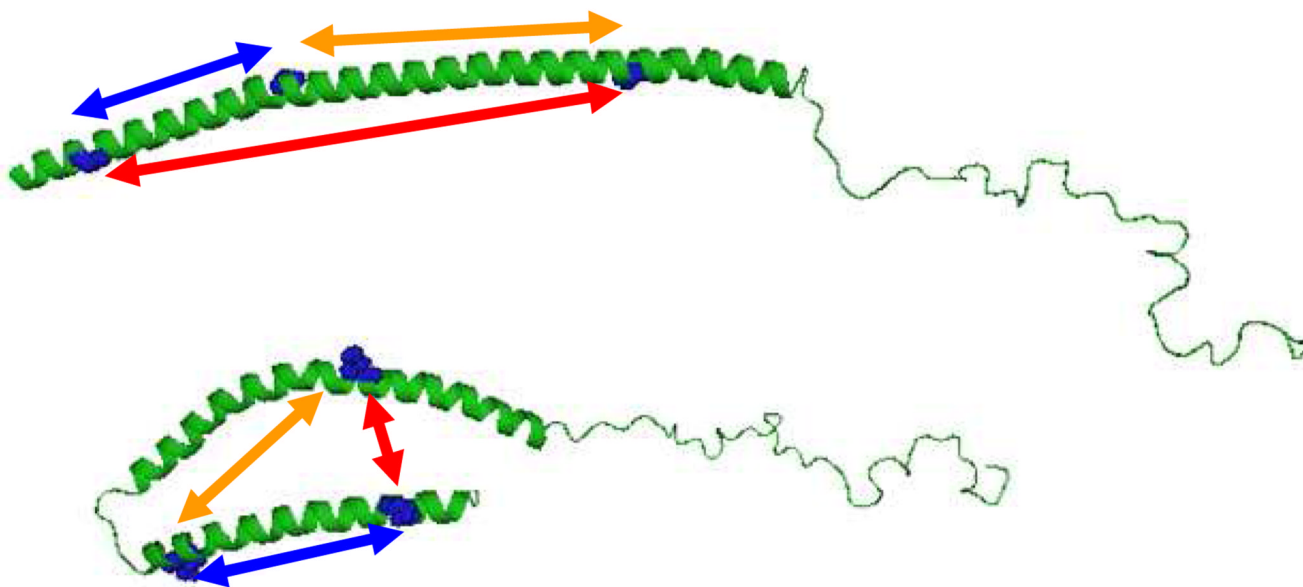36. Volles MJ, Lansbury PT. Biochemistry 2002;41:4595–4602. [PubMed: 11926821]

Figure 1.
Possible configurations of membrane-bound AS. Bottom, bent-helix model, from NMR structure of AS on SDS micelles (PDB: 1XQ8). Top, elongated helix model (cartoon from PyMol). Mutations for labeling are shown as blue spheres. Arrows on both molecules are color-matched to show the expected relative distances compared with the three AS FRET constructs described in the text: AS-S9C-T72C (red), AS-T33C-T72C (yellow), AS-S9C-T33C (blue). All mutations are in the helix-forming region (residues 1–90) and FRET between these locations distinguishes between these possible structural models
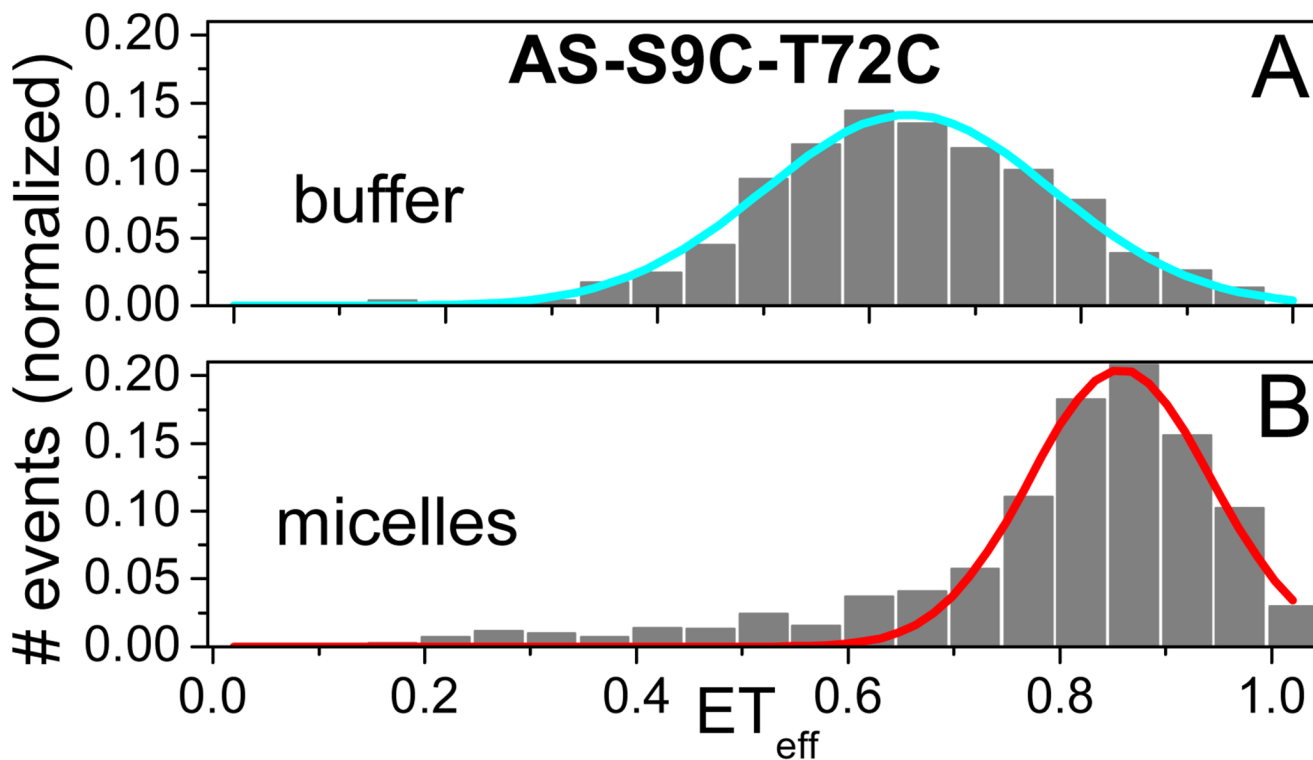
Figure 2.
ET_{eff} histograms of AS-S9C-T72C in buffer (A) or in the presence of 40 mM SDS (B). Each histogram contains >2000 events. The high ET_{eff} observed in the micelle bound form of AS indicates that residues 9 and 72 are brought into close proximity, as expected based on the model illustrated in Figure 1. The lack of measurable energy transfer for the vesicle bound protein (not shown) suggests that the protein takes a more extended conformation when bound to vesicles.
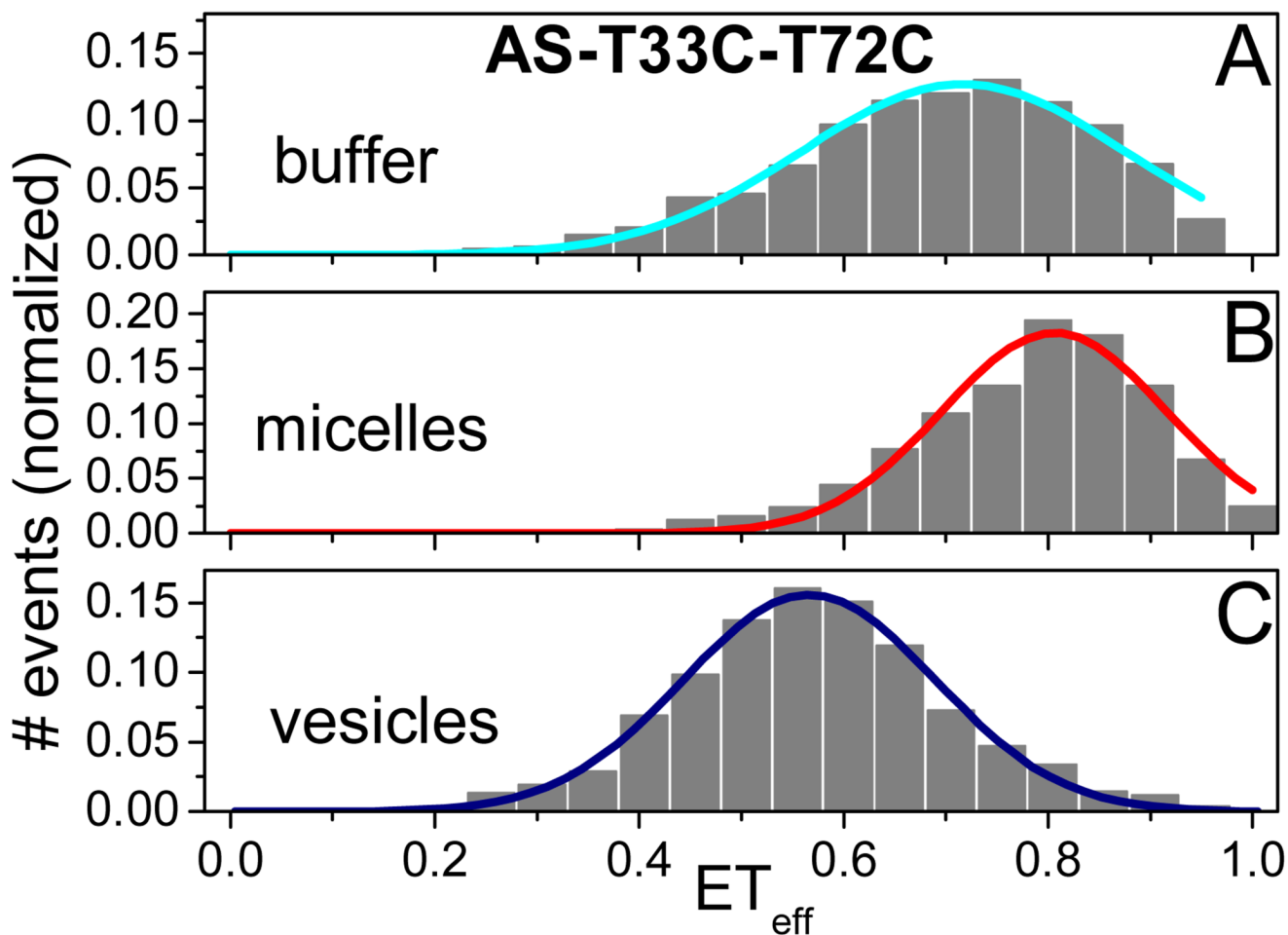
Figure 3.
ET_{eff} histograms of AS-T33C-T72C in buffer (A) or in the presence of 40 mM SDS (B) or 160 µM POPS (C). In contrast to AS-S9C-T72C, we are able to observe three distinct conformations in the three measurement conditions for this construct. Of primary importance is that this data distinguishes between the micelle bound (B) and vesicle bound (C) conformations of AS and supports that the vesicle bound protein is more extended (Figure 1).